A TIM-Based Neutron Temporal Diagnostic for Cryogenic Experiments on OMEGA

Introduction

In inertial confinement fusion[1] experiments, shells filled with deuterium (D_2) or a deuterium–tritium (DT) mixture are heated by either direct laser illumination or soft x-ray radiation in a laser-heated hohlraum. The target is compressed to conditions under which thermonuclear fusion occurs. The most-promising target designs consist of a layered cryogenic D_2 or DT shell enclosed by a very thin shell of plastic, which is ablated very early and does not contribute significantly to the dynamics of the implosion.[2,3] During the plasma confinement time, which is of the order of 100 ps, fuel atoms undergoing fusion release energetic charged particles, photons, and neutrons. The fusion reactions of interest are

$$\begin{aligned} &\mathrm{D} + \mathrm{D} \rightarrow \mathrm{n}\ (2.45\ \mathrm{MeV}) + {}^{3}\mathrm{He}\ (0.82\ \mathrm{MeV}), \\ &\mathrm{D} + \mathrm{D} \rightarrow \mathrm{p}\ (2.5\ \mathrm{MeV}) + \mathrm{T}\ (1.01\ \mathrm{MeV}), \qquad (1) \\ &\mathrm{T} + \mathrm{D} \rightarrow \alpha\ (3.5\ \mathrm{MeV}) + \mathrm{n}\ (14.1\ \mathrm{MeV}). \end{aligned}$$

The particle energies are shown in parentheses. While most of the charged particles are slowed down in the plasma and stopped, or "ranged out," before they leave the target, most neutrons escape the fuel without collision. As a result, the time history of neutrons arriving at an external diagnostic represents the burn history of the target fuel. Measurements of the neutron burn history provide important information about target performance that can be compared directly with numerical models. The time of peak neutron emission—the "neutron bang time"—is very sensitive to the details of the energy absorption and the equation of state used to describe the plasma. The neutron burn history contains valuable information about the plasma evolution close to the peak of compression. Target and laser illumination nonuniformities can feed through to the inner surface of the shell by the deceleration phase. Amplified by the Rayleigh–Taylor growth, these nonuniformities can severely disrupt the hot, neutron-producing region of the target, leading to a strongly distorted neutron burn history. Several detectors measuring the neutron bang time[4–8] are described in the literature, but only the streak-camera–based neutron temporal diagnostic[9] (NTD) is capable of resolving the details of the neutron burn history with a resolution of ~50 ps for DD neutrons and ~25 ps for DT neutrons. The NTD is currently installed on LLE's OMEGA laser. NTD is a highly successful instrument,[10] but the size of the cryogenic target shroud system prevents placing the scintillator of the NTD system at its optimum location close to the target. This makes it too insensitive to record the burn history of the current D_2 cryogenic target experiments. Furthermore, Doppler broadening of the neutron spectrum severely compromises the time resolution of NTD at larger distances.[9] These mechanical constraints motivated the development of new cryogenic-compatible neutron temporal diagnostic (cryoNTD), which fits into LLE's standard ten-inch manipulator (TIM) diagnostic inserters, to provide high-resolution neutron emission measurements for cryogenic implosions. This article describes the setup of cryoNTD and first experimental results compared to NTD on room-temperature direct-drive implosions and on cryogenic implosions.

Setup of the Detector System

The cryoNTD system, shown schematically in Fig. 92.6, is based on a fast plastic scintillator (Bicron BC422[11]), which converts the kinetic energy of the neutrons into light. A light collection and transfer system (Fig. 92.7) transports the light from the scintillator to the input plane of a fast (<15-ps) optical streak camera.[12] The front end of the optical system is mounted in the TIM and inserted close to the target. An optical fiducial is used to time the neutron signals relative to the incident laser pulse. The size of the scintillator is that required to record high-quality burn histories at a yield comparable to 10^{10}, which is the performance of the early cryogenic D_2 target implosions on OMEGA.[3] A simple scaling from the sensitivity of NTD with a 6-mm-diam scintillator at 2 cm from the target to the required standoff distance of 9 cm shows that a 30-mm-diam scintillator is sufficient. Due to the limited size of the photocathode of the streak camera, a demagnifying optical system

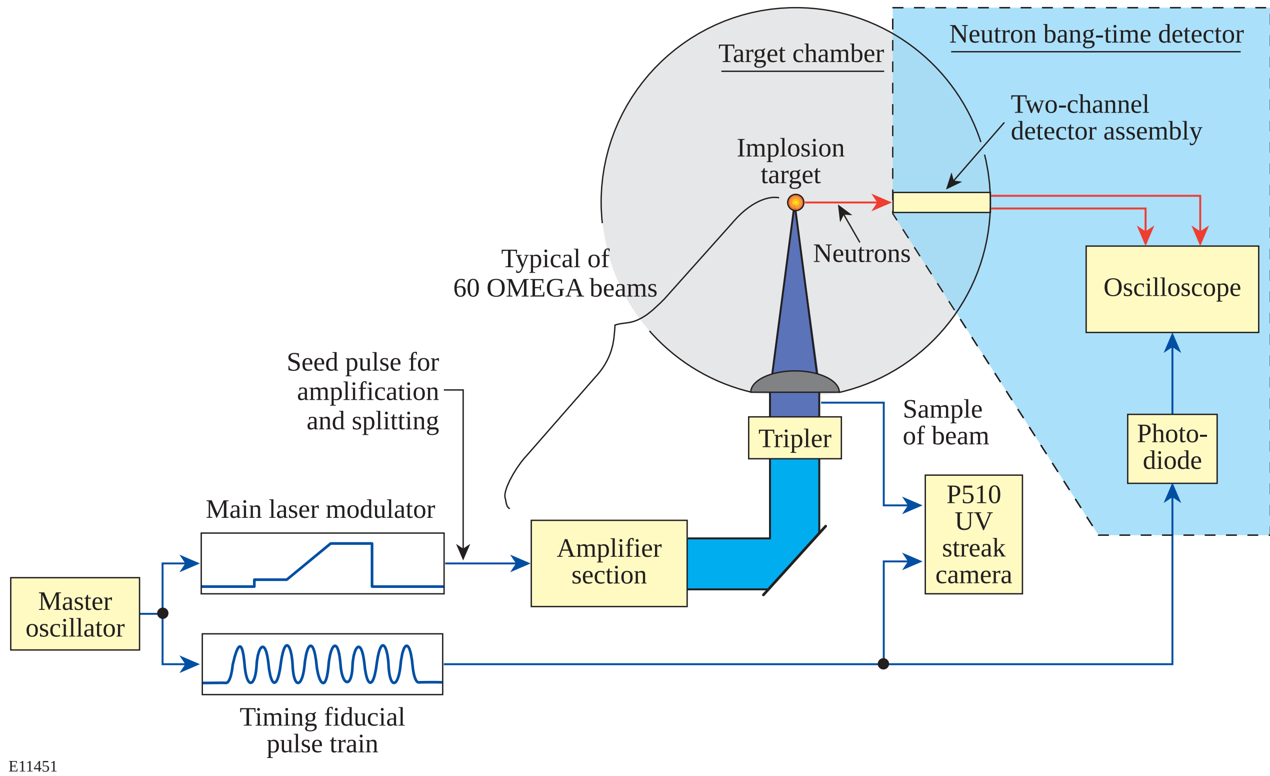

Figure 92.6
A block diagram of the cryoNTD detector system integrated into the OMEGA facility. The fiducial system provides cross timing between the neutron signals and the incident laser pulse, which is recorded on the P510 UV streak camera.

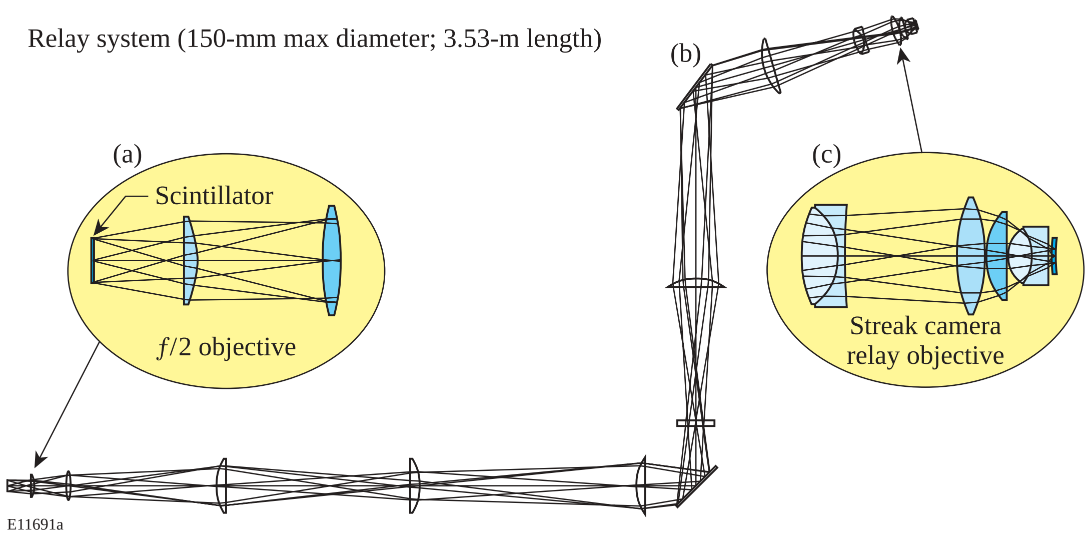

Figure 92.7
A fast scintillator converts the neutron kinetic energy into light, which is collected by a fast *f*/2 optic (a). An optical system (b) transports the light to the input plane of a fast optical streak camera with 3:1 demagnification though an *f*/0.67 final lens system (c).

with a 3:1 ratio is used. A fast *f*/2 lens collects the light from the scintillator with high efficiency [Fig. 92.7(a)]. An optical system consisting of 11 lenses and 2 mirrors relays the image of the scintillator though the TIM and the vacuum window along a 3.5-m optical path to the streak camera [Fig. 92.7(b)]. The 3:1 demagnification in combination with the fast *f*/2 lens leads to a very demanding *f*/0.67 final lens system, which maximizes the transmission of the optical system [Fig. 92.7(c)]. The 527-nm light from the OMEGA fiducial system is delivered via an optical fiber collimated and imaged onto the streak camera through the final lens assembly. The OMEGA fiducial consists of a series of eight pulses spaced 548 ps apart and is synchronized to the shaped OMEGA laser pulse with a jitter of less than 20 ps. The optical fiducial is amplified separately from the main laser pulse, split, and distributed to various diagnostic instruments for precision timing. The fiducial pulse train is also recorded on the P510 ultraviolet streak camera,[13] which measures the laser pulse shape. The common optical fiducial serves as a reference for both the neutron signal and the laser pulse, thus enabling very accurate timing of the cryoNTD signals.

The low light levels from the scintillator, the fast collection and transport optic, and the TIM design make it necessary to install a sophisticated system of shields and light baffles to avoid any scattered laser light from entering the optical system. Figure 92.8(a) shows a sample image from a cryogenic D_2 implosion with a yield of 3.17×10^{10} recorded on the CCD camera attached to the optical streak camera. The fiducial is seen on top of the image and the scintillator output in the center. The "wings" seen on either side of the scintillator signal are most probably produced by the spatially nonuniform transmission of the optical system. Figure 92.8(b) shows image exposure versus time averaged across the central portion of the scintillator signal. The streak camera flat-field and geometric distortions are included in the signal processing. The time history of the scintillator signal is the convolution of the neutron temporal distribution with the scintillator response. The scintillator has a very fast rise time of <20 ps and a decay time of ~1.2 ns. Consequently the burn history information is encoded in the leading edge of the pulse due to the much longer decay of the scintillator compared to the burnwidth.

Data Analysis and Calibration

The actual neutron burn history is obtained by deconvolving the effect of the long scintillator decay from the recorded signal. A "physical modeling" approach is used for the deconvolution, where the neutron signal n_i at the pixel location i is given as the recorded signal s_i minus the sum of all earlier neutron signals, which are decaying exponentially at the scintillator fall time τ:

$$n_i = s_i - \sum_{j=0}^{i-1} n_j \exp\left[\frac{(i-j)\times \Delta t_p}{\tau}\right]. \qquad (2)$$

In this equation, Δt_p is the time separation of two pixels. This method is fast and deterministic and is very stable against noise on the streak camera signal. The neutron signal is broadened by several different mechanisms. The thermal broadening of the neutron energy spectrum leads to an arrival time spread in the scintillator of[9]

$$\Delta t_T^{\mathrm{DD}} = 778 \frac{\mathrm{ps}}{m\ \mathrm{keV}^{1/2}} \sqrt{T} \times d \qquad (3)$$

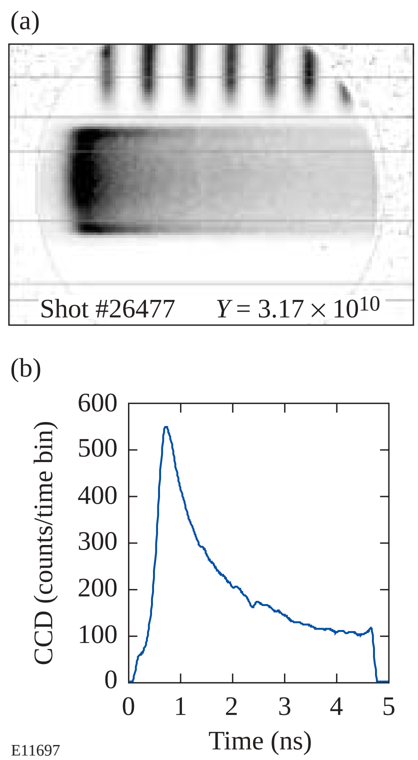

Figure 92.8
A streak camera image (a) of the neutron signal from a D_2 cryogenic implosion with a yield of 3.17×10^{10}. The fiducial seen on the top of the image is used for timing the neutron signal to the incident laser pulse. The image exposure versus time (b) is averaged across the central portion of the scintillator signal.

for DD neutrons, where Δt_T is the FWHM in ps, d is the target-to-detector distance in meters, and T is the neutron-averaged ion temperature in keV. For the 9-cm standoff distance of cryoNTD, this effect limits the time resolution to ~70 ps at 1 keV. The finite neutron transit time through the scintillator $\Delta t_s = \Delta x / v_n$ broadens the signal by $\Delta t_s^{\mathrm{DD}} = 44$ ps with a 1-mm-thick scintillator using a neutron speed of v_n = 2.16 cm/ns. Adding both effects in quadrature gives an estimate of ~80 ps for the time resolution of cryoNTD. Figure 92.9 shows a comparison of the neutron burn histories obtained by NTD and cryoNTD on a room-temperature direct-drive OMEGA plastic target filled with 15 atm of D_2. The signals are aligned in time for best correlation to allow a better comparison. Although the effects of the limited time resolution of cryoNTD compared to NTD, which has a time resolution of ~50 ps for DD neutrons, can be seen, the burn histories compare very favorably.

Absolute timing is established using the OMEGA fiducial system. The recorded fiducial pulse is fitted by a pulse train of eight Gaussian pulses spaced apart at the well-characterized period of d_t = 548 ps:

$$\mathrm{fidu}(t) = \sum_{i=0}^{7} a_i \exp\left\{-\left[t-\left(t_0 + i \times dt\right)\right]^2 \Big/ 2\sigma^2\right\} \qquad (4)$$

to the recorded signal. Here a_i is the amplitude of each fiducial peak, t_0 is the time of the first fiducial pulse, and σ is the standard deviation of an individual fiducial pulse. This reduces the influence of noise on the determination of the timing reference. CryoNTD has been calibrated against NTD using a series of room-temperature plastic targets filled with D_2. The bang times measured by cryoNTD are very close to the bang times from NTD (Fig. 92.10), showing only 40-ps rms spread. Figure 92.11 shows a comparison of neutron burn histories from a direct-drive cryogenic target with a low-nonuniformity ice layer[3] and a cryogenic target with a very poor layer quality, both irradiated by a 1-ns, square, 23-kJ laser

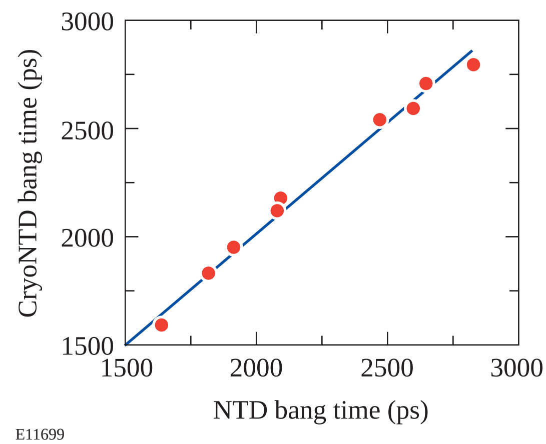

Figure 92.10
The bang times measured by the NTD compared to those of the cryoNTD for a series of room-temperature plastic targets.

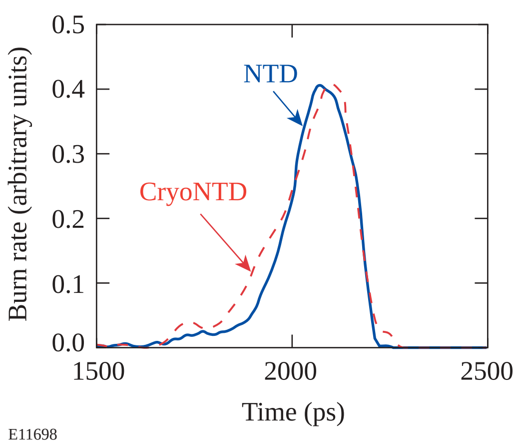

Figure 92.9
A comparison of the neutron burn histories recorded by the cryoNTD and the NTD from a room-temperature plastic target filled with 15 atm D_2 at a yield of 2×10^{10}.

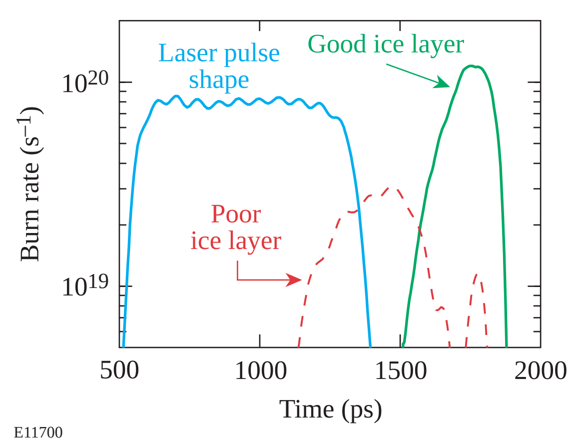

Figure 92.11
A comparison of neutron burn histories from direct-drive cryogenic targets with a good ice layer (solid line) and a poor ice layer (dashed line). Both targets are driven by a 1-ns square laser pulse.

pulse. The temporal shape of the laser pulse is shown for comparison. Even though the neutron yield of both implosions is relatively close—1.5×10^{10} for the poor capsule and 3.1×10^{10} for the good capsule—the neutron burn history shows dramatic differences.

Summary and Outlook

A cryogenic-compatible neutron temporal diagnostic (cryoNTD) has been developed for OMEGA to allow the high-resolution measurement of the neutron burn history on early direct-drive D_2 cryogenic targets. The scintillator and the front end of the optical system are mounted in a TIM and inserted close to the target. The back end of the optical system containing the optical streak camera to record the light emitted from the scintillator is mounted outside the vacuum of the target chamber. The OMEGA fiducial system is used to cross-time the neutron signals to the incident laser pulse. This instrument is able to measure the neutron burn history at yields $>10^9$ DD neutrons with a resolution of ~80 ps. An absolute timing accuracy of 40 ps has been demonstrated using cross-calibration to the NTD. The time resolution of the cryoNTD is sufficient to resolve the important features of the reaction rate history of cryogenic implosions with high absolute timing accuracy. Future optimized cryogenic targets will generally show higher neutron yields,[3] allowing the use of a thinner scintillator (<0.5 mm), which will improve the time resolution of the instrument. Neutral density filters can be inserted in the light path to accommodate even the highest predicted yields, which will be comparable to 10^{12}.

ACKNOWLEDGMENT

This work was supported by the U.S. Department of Energy Office of Inertial Confinement Fusion under Cooperative Agreement No. DE-FC03-92SF19460, the University of Rochester, and the New York State Energy Research and Development Authority. The support of DOE does not constitute an endorsement by DOE of the views expressed in this article.

REFERENCES

1. J. H. Nuckolls, Phys. Today **35**, 24 (1982).
2. S. Skupsky, R. Betti, T. J. B. Collins, V. N. Goncharov, D. R. Harding, R. L. McCrory, P. W. McKenty, D. D. Meyerhofer, and R. P. J. Town, in *Inertial Fusion Sciences and Applications 2001*, edited by K. Tanaka, D. D. Meyerhofer, and J. Meyer-ter-Vehn (Elsevier, Paris, 2002), pp. 240–245.
3. C. Stoeckl, C. Chiritescu, J. A. Delettrez, R. Epstein, V. Yu. Glebov, D. R. Harding, R. L. Keck, S. J. Loucks, L. D. Lund, R. L. McCrory, P. W. McKenty, F. J. Marshall, D. D. Meyerhofer, S. F. B. Morse, S. P. Regan, P. B. Radha, S. Roberts, T. C. Sangster, W. Seka, S. Skupsky, V. A. Smalyuk, C. Sorce, J. M. Soures, R. P. J. Town, J. A. Frenje, C. K. Li, R. D. Petrasso, F. H. Séguin, K. Fletcher, S. Padalino, C. Freeman, N. Izumi, R. Lerche, and T. W. Phillips, Phys. Plasmas **9**, 2195 (2002).
4. R. A. Lerche *et al.*, Rev. Sci. Instrum. **59**, 1697 (1988).
5. N. Miyanaga *et al.*, Rev. Sci. Instrum. **6**, 3592 (1990).
6. R. A. Lerche, M. D. Cable, and D. W. Phillion, Rev. Sci. Instrum. **61**, 3187 (1990).
7. T. J. Murphy and R. A. Lerche, *ICF Quarterly Report* **3**, 35, Lawrence Livermore National Laboratory, Livermore, CA, UCRL-LR-105821-93-1 (1992).
8. R. A. Lerche, D. W. Phillion, and G. L. Tietbohl, in *Ultrahigh- and High-Speed Photography, Videography, and Photonics '93*, edited by P. W. Roehrenbeck (SPIE, Bellingham, WA, 1993), Vol. 2002, pp. 153–161.
9. R. A. Lerche, D. W. Phillion, and G. L. Tietbohl, Rev. Sci. Instrum. **66**, 933 (1995).
10. D. D. Meyerhofer, J. A. Delettrez, R. Epstein, V. Yu. Glebov, V. N. Goncharov, R. L. Keck, R. L. McCrory, P. W. McKenty, F. J. Marshall, P. B. Radha, S. P. Regan, S. Roberts, W. Seka, S. Skupsky, V. A. Smalyuk, C. Sorce, C. Stoeckl, J. M. Soures, R. P. J. Town, B. Yaakobi, J. D. Zuegel, J. Frenje, C. K. Li, R. D. Petrasso, D. G. Hicks, F. H. Séguin, K. Fletcher, S. Padalino, M. R. Freeman, N. Izumi, R. Lerche, T. W. Phillips, and T. C. Sangster, Phys. Plasmas **8**, 2251 (2001).
11. Bicron Newbury, Newbury, OH 44065-9577.
12. R. A. Lerche, in *Ultrahigh- and High-Speed Photography, Videography, Photonics, and Velocimetry '90*, edited by P. A. Jaanimagi, B. T. Neyer, and L. L. Shaw (SPIE, Bellingham, WA, 1991), Vol. 1346, pp. 376–383.
13. W. R. Donaldson, R. Boni, R. L. Keck, and P. A. Jaanimagi, Rev. Sci. Instrum. **73**, 2606 (2002).